



Integrated design of robotic mechanisms for force balancing and trajectory tracking

P.R. Ouyang^a, Q. Li^b, W.J. Zhang^{a,*}

^a *Advanced Engineering Design Laboratory (AEDL), Department of Mechanical Engineering, University of Saskatchewan, 57 Campus Drive, Saskatoon, SK, Canada S7N 5A9*

^b *Division of Systems and Engineering Management, School of Mechanical and Production Engineering, Nanyang Technological University, Singapore*

Received in revised form 28 February 2002; accepted 20 March 2002

Abstract

Traditionally, mechanisms are driven by constant velocity motors. A real-time controllable (RTC) mechanism refers to the mechanism driven by servomotors, which can be planned and scheduled in real-time. Robot manipulators are typical examples of the RTC mechanisms. The generic task of an RTC mechanism is the trajectory or motion tracking. This paper describes an integrated approach to design an RTC mechanism considering force balancing and trajectory tracking, simultaneously. In particular, a new approach called adjusting kinematic parameter (AKP) for the force balancing of RTC mechanisms is described. The force balanced mechanism has simpler dynamics, and thus facilitates the development of control systems for performing trajectory tracking. This paper demonstrates that the force balanced mechanism by the AKP approach is more promising than those by other approaches in terms of the reduction of joint forces and torques in servomotors, and improvement of the trajectory tracking performance. Based on simulation, this paper also shows the effects of two different control systems: PD and non-linear PD versus the AKP approach and the counterweight approach.

Crown Copyright © 2003 Published by Elsevier Science Ltd. All rights reserved.

Keywords: Controllable mechanism; Force balancing; Trajectory tracking; PD/NPD control

* Corresponding author. Tel.: +1-306-966-5478; fax: +1-306-966-5427.

E-mail addresses: puo545@mail.usask.ca (P.R. Ouyang), mqli@ntu.edu.sg (Q. Li), chris_zhang@engr.usask.ca (W.J. Zhang).

1. Introduction

Prior to the advent of the modern electronics technology, mechanisms usually used motors that are not real-time controllable (RTC). Such mechanisms can assure the coordination of different output motions and high efficiencies in energy consumption, and can be designed to satisfy high-speed mass production. The main disadvantage of these mechanisms is their lack of flexibility in applications, as a change in the output motions requires a corresponding change in the dimensions of the mechanism.

The advent of high performance real-time adjustable motors makes it possible to produce different output motions with the same physical setup of a mechanism only by changing some parameters in the control program. A mechanism can be used in more diversified applications when it is equipped with servomotors. A typical example of the servomotor concept is a robotic manipulator, where each link (or some links) of the robot is driven by a servomotor to produce flexible motions under various payloads. Motions generated by the servomotors can be adjusted with either off-line or on-line programs. These programs for changing parameters related to electronic signals and their relevant hardware are called the controller for short in this paper. It should be noticed that the generic task of servomotor driven machines can be concluded as “trajectory tracking” [3].

For mechanisms, complete force balancing is a basic problem [1,4,6,8–11]. Whenever an unbalanced mechanism runs, the shaking force is transmitted to its surroundings as a sort of disturbances. This disturbance causes vibration, noise, wear, and fatigue, as well as large energy consumption problems, and therefore limits the full potential of many mechanisms. The force balancing of the mechanism attempts to keep the center of the mass of the mechanism stationary under any configuration so that the resultant of the inertia forces, namely, the shaking force, can be cancelled.

The first study of complete force balancing of mechanisms was the method of “mass redistribution” proposed by Berkof and Lowen [1], with which additional masses were “added” into a force unbalanced mechanism. This method is also called the counterweight (CW) method. Due to the added CWs, the magnitude of the forces acted in each link is likely greater than those before the balancing. The disadvantage with this method is the increases of both the rotating inertia and the total system mass. It was found that at higher speeds, the performance of mechanisms, trajectory tracking, is degraded [7]. Another method to balance the shaking force is the use of the springs [6]. But the complete force balancing of the mechanism using springs is possible only in one direction, i.e., the gravity direction. Furthermore, the fatigue problem of springs cannot be neglected, and it sometimes has significant effects on the mechanism life. Another problem of using springs may be the complexity in designing a control algorithm for real-time feedback control applications because the spring will contribute to the dynamics of a system [14]. Although a so-called zero reaction mechanism was designed based on the redundant actuators [10], in such a mechanism, additional actuators are added into the mechanism. The addition of kinematically redundant actuators leads to the complexity in designing controllers,

and indeed how these redundant actuators affect the trajectory tracking performance was not addressed. It is obvious that such systems bear high cost and have a limited application domain because the structure of the systems is of parallelogram. For instance, it is shown that the system has a much smaller workspace [10].

Simultaneous consideration of the design of the mechanical structures and the design of the controller, or the integrated design and control of mechanisms, in light of improving both shaking force cancellation and trajectory tracking, is studied generally in an ad-hoc manner. Youcef-Toumi and Kuo [12] discovered that the dynamic equation was completely decoupled by adding a parallelogram structure on a two-link open-chain mechanism, which led to a closed-loop parallelogram five-bar mechanism; this thus led to the improvement of the positioning accuracy with their system. Such systems also coincidentally cancelled the shaking force. Chuenchom and Kota [2] presented an analytical method for designing adjustable mechanisms based on the synthesis of adjustable dyads. In their paper, only the kinematic analysis was performed and the mechanism was programmed off-line. Neither the dynamic control nor the force balancing issue was addressed.

It is interesting to notice that all the methods for force balancing or moment balancing were initiated for traditional mechanisms without the possibility of on-line adjusting or real-time control. Therefore, a research question arises: whether can a novel method for force balancing directed to RTC mechanisms be developed? With such a method, the performance of trajectory tracking is also improved, and some disadvantages associated with the CW approach for force balancing could be eliminated.

The objective of this paper is to develop a novel approach for force balancing and the facilitation of the design of controllers (which further leads to the improvement of trajectory tracking performance). This approach is called adjusting kinematic parameter (AKP). The AKP approach works only for RTC mechanisms. The paper is organized as follows. The AKP approach is described in Section 2. In Section 3, a simulation system for the example mechanism that is a closed-loop five-bar mechanism with two degrees of freedom (DOF) is described. Section 4 shows the following simulation results: (i) comparison of the unbalanced mechanism, the balanced mechanism with the CW approach, and the balanced mechanism with the AKP approach in terms of the joint reaction force and trajectory tracking performance under different operating situations, and (ii) comparison of two different controllers, the PD controller and the non-linear PD controller. A conclusion with future work is presented in Section 5.

2. The AKP approach

Without losing the generality, a closed loop mechanism, as shown in Fig. 1, is used for the illustration purpose. This mechanism has two DOFs and requires two driving motors. The two driving motors are usually placed on the fixed link (called the center link) to drive the two input links connected to the frame. Assume the two motors here are servomotors. The mechanism is thus an RTC mechanism.

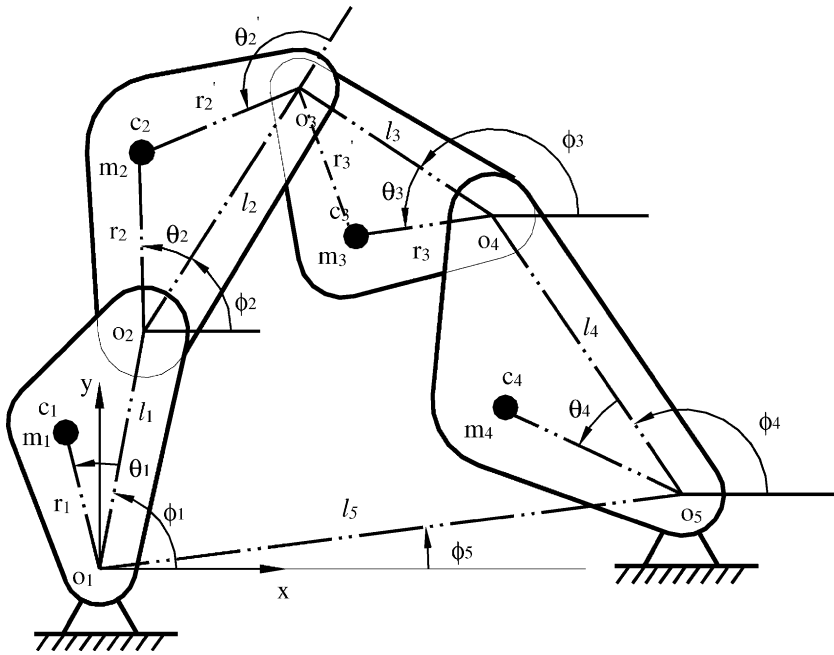


Fig. 1. A closed-loop five-bar mechanism with arbitrary mass distribution.

2.1. Conditions for stationary total mass center of a system

Let \mathbf{f}_0 stand for the sum of the reacting forces the ground imposes to the mechanism. According to the Newton’s second law, we have

$$\mathbf{f}_0 = -\frac{d}{dt}\{M\dot{\mathbf{r}}_c\} + Mg \tag{1}$$

where M is the total mass of the mechanism, g is the acceleration of gravity vector, and $\dot{\mathbf{r}}_c$ is the velocity of the center of mass (CM) of the system. It can be seen from Eq. (1) that \mathbf{f}_0 has an undesired dynamic component resulting from the changes in the system’s linear momentum, and a static component due to gravity. The dynamic components in Eq. (1) are zero if the CM does not change in any configuration, i.e., $\mathbf{r}_c = \mathbf{constant}$. For the closed-loop five-bar mechanism in Fig. 1, we have:

$$\mathbf{r}_c = \frac{1}{M} \sum_{i=1}^4 m_i \mathbf{r}_{ci} = \mathbf{constant} \tag{2}$$

where $M = \sum_{i=1}^4 m_i$, m_i and \mathbf{r}_{ci} are the mass and the position vector of mass center of link i , respectively.

In order to derive the conditions for force balancing, we need to express explicitly in terms of those time-varying quantities. The linearly independent-vector method [1] is used to rewrite Eq. (2).

From Fig. 1, the position vectors \mathbf{r}_{ci} in Eq. (2) can be expressed as:

$$\begin{cases} \mathbf{r}_{c1} = r_1 \mathbf{e}^{i(\phi_1 + \theta_1)} \\ \mathbf{r}_{c2} = l_1 \mathbf{e}^{i\phi_1} + r_2 \mathbf{e}^{i(\phi_2 + \theta_2)} \\ \mathbf{r}_{c3} = l_3 \mathbf{e}^{i\phi_5} + l_4 \mathbf{e}^{i\phi_4} + r_3 \mathbf{e}^{i(\phi_3 + \theta_3)} \\ \mathbf{r}_{c4} = l_5 \mathbf{e}^{i\phi_5} + r_4 \mathbf{e}^{i(\phi_4 + \theta_4)} \end{cases} \quad (3)$$

Substituting Eq. (3) into Eq. (2) yields:

$$\begin{aligned} M\mathbf{r}_c = & (m_3 l_5 \mathbf{e}^{i\phi_5} + m_4 l_5 \mathbf{e}^{i\phi_5}) + (m_1 r_1 \mathbf{e}^{i\theta_1} + m_2 l_1) \mathbf{e}^{i\phi_1} + (m_2 r_2 \mathbf{e}^{i\theta_2}) \mathbf{e}^{i\phi_2} \\ & + (m_3 r_3 \mathbf{e}^{i\theta_3}) \mathbf{e}^{i\phi_3} + (m_4 r_4 \mathbf{e}^{i\theta_4} + m_3 l_4) \mathbf{e}^{i\phi_4} \end{aligned} \quad (4)$$

The unit vectors $\mathbf{e}^{i\phi_1}$, $\mathbf{e}^{i\phi_2}$, $\mathbf{e}^{i\phi_3}$, and $\mathbf{e}^{i\phi_4}$ are subjected to a constraint derived from the kinematic closed-loop equation, i.e.,

$$l_1 \mathbf{e}^{i\phi_1} + l_2 \mathbf{e}^{i\phi_2} - l_3 \mathbf{e}^{i\phi_3} - l_4 \mathbf{e}^{i\phi_4} - l_5 \mathbf{e}^{i\phi_5} = 0 \quad (5)$$

Substituting Eq. (5) into Eq. (4) yields:

$$\begin{aligned} M\mathbf{r}_c = & (m_3 l_5 \mathbf{e}^{i\phi_5} + m_4 l_5 \mathbf{e}^{i\phi_5} + \lambda_{25} m_2 r_2 \mathbf{e}^{i\theta_2} \mathbf{e}^{i\phi_5}) + (m_1 r_1 \mathbf{e}^{i\theta_1} + m_2 l_1 - \lambda_{21} m_2 r_2 \mathbf{e}^{i\theta_2}) \mathbf{e}^{i\phi_1} \\ & + (m_3 r_3 \mathbf{e}^{i\theta_3} + \lambda_{23} m_2 r_2 \mathbf{e}^{i\theta_2}) \mathbf{e}^{i\phi_3} + (m_4 r_4 \mathbf{e}^{i\theta_4} + m_3 l_4 + \lambda_{24} m_2 r_2 \mathbf{e}^{i\theta_2}) \mathbf{e}^{i\phi_4} \end{aligned} \quad (6)$$

where $\lambda_{ij} = l_j/l_i$, $i, j = 1, \dots, 5$. Coefficients of all terms with time-varying quantities in Eq. (6) with only linear independent terms should vanish. This leads to the following equations:

$$m_1 r_1 \mathbf{e}^{i\theta_1} + m_2 l_1 - \lambda_{21} m_2 r_2 \mathbf{e}^{i\theta_2} = 0 \quad (7)$$

$$m_3 r_3 \mathbf{e}^{i\theta_3} + \lambda_{23} m_2 r_2 \mathbf{e}^{i\theta_2} = 0 \quad (8)$$

$$m_4 r_4 \mathbf{e}^{i\theta_4} + m_3 l_4 + \lambda_{24} m_2 r_2 \mathbf{e}^{i\theta_2} = 0 \quad (9)$$

Using the relationships $r_2 \mathbf{e}^{i\theta_2} = l_2 + r'_2 \mathbf{e}^{i\theta'_2}$ and $r_3 \mathbf{e}^{i\theta_3} = l_3 + r'_3 \mathbf{e}^{i\theta'_3}$, we can obtain the force balancing conditions for the closed-loop five-bar mechanism as follows:

$$m_1 r_1 l_2 = l_1 m_2 r'_2 \quad \text{and} \quad \theta_1 = \theta'_2 \quad (10)$$

$$m_3 r_3 l_2 = l_3 m_2 r_2 \quad \text{and} \quad \theta_3 = \pi + \theta_2 \quad (11)$$

$$m_4 r_4 l_3 = l_4 m_3 r'_3 \quad \text{and} \quad \theta_4 = \theta'_3 \quad (12)$$

When a system is not designed as force balanced one, we can add masses, or counterweights, to the system, and this is the CW approach [1]. The added mass can be calculated with the equations listed in Appendix A.

2.2. *AKP principle and its design equations*

Careful examining of Eqs. (10)–(12) also shows the possibility to satisfy the balancing conditions by changing kinematic parameters, l_i , ($i = 1, 2, 3, 4$). It should be noticed that the change of l_i also changes r_i and θ_i . This is the basic idea of the AKP approach. The design equations for the AKP approach are derived as follows:

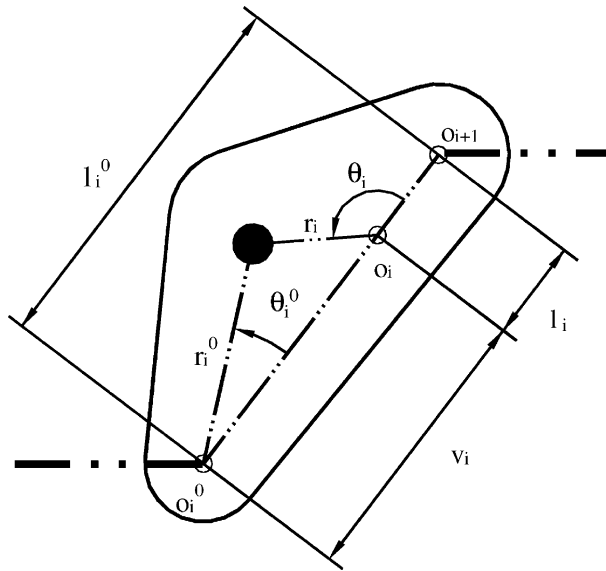


Fig. 2. The principle of the AKP approach.

In Fig. 2, l_i^0 represents the length of link i before adjusting Pivot o_i^0 , and (r_i^0, θ_i^0) represents the position of the mass center of link i . After adjusting pivot from o_i^0 to o_i , l_i represents the length of link i , (r_i, θ_i) for the new position of the mass center, and v_i is the distance that the pivot is adjusted. Using the AKP approach, adjusting the pivots of some links, the following equations can be derived.

$$l_i = l_i^0 - v_i \tag{13}$$

$$r_i^0 \cos \theta_i^0 = v_i + r_i \cos \theta_i \tag{14}$$

where $i = 1, 2, 3, 4$. If the pivot of Link 2 is selected to be unchanged, the force balanced mechanism can be achieved by adjusting the pivot positions of the other three moving links. Substituting Eqs. (13) and (14) into Eqs. (10)–(12) yields:

$$v_1 = (m_2 r_2' l_1^0 \cos \theta_1 - m_1 r_1^0 l_2 \cos \theta_1^0) / (m_2 r_2' \cos \theta_1 - m_1 l_2) \tag{15}$$

$$v_3 = (m_2 r_2 l_3^0 \cos \theta_3 - m_3 r_3^0 l_2 \cos \theta_3^0) / (m_2 r_2 \cos \theta_3 - m_3 l_2) \tag{16}$$

$$v_4 = (k l_4^0 \cos \theta_4 - m_4 r_4^0 \cos \theta_4^0) / (k \cos \theta_4 - m_4) \tag{17}$$

where

$$k = \sqrt{(m_2 r_2 / l_2)^2 + m_3^2 + (2 m_2 r_2 m_3 \cos \theta_2 / l_2)}$$

It should be noticed that for a given task, i.e., a set of trajectory points, through the inverse kinematics, the corresponding motor angles corresponding with the given task can be calculated. The inverse kinematic relationship depends on the kinematic parameters. After applying the AKP approach for force balancing, the kinematic

parameters are changed. To maintain the fulfillment of the same trajectory tracking task, a new set of motor angles should be found. The possibility of this adjusting process can only be provided by the RTC motors. This is the reason why the AKP approach is only applicable to the RTC mechanisms.

To verify the AKP approach, a model of the closed-loop five-bar mechanism is built with lego blocks, shown in Fig. 3. Fig. 3(a) shows the unbalanced system. After applying the AKP approach, the kinematic parameters are reset. Fig. 3(b) and (c) show, respectively, two configurations of the balanced system. They can rest at these two positions and also any other positions, which means that the system is force balanced.

3. The simulation system

A simulation system is needed to develop understanding of the benefits of the AKP approach. The simulation system includes: (i) the dynamic model of the closed-loop five-bar mechanism, (ii) the inverse kinematic model, (iii) the motion planning model, and (iv) the control models. These models are briefly introduced in the following.

3.1. The dynamic model

Generally, in the absence of friction and other disturbances, the dynamic model of the closed-loop five-bar mechanism can be written as:

$$\mathbf{M}(\mathbf{q})\ddot{\mathbf{q}} + \mathbf{F}(\mathbf{q}, \dot{\mathbf{q}})\dot{\mathbf{q}} + \mathbf{G}(\mathbf{q}) = \mathbf{T}(\mathbf{t}) \quad (18)$$

where $\mathbf{q}(\mathbf{t}) \in \mathcal{R}^{2 \times 1}$ is the vector of the joint angular positions, $\mathbf{T}(\mathbf{t}) \in \mathcal{R}^{2 \times 1}$ is the vector of applied joint torques, $\mathbf{M}(\mathbf{q}) \in \mathcal{R}^{2 \times 2}$ the symmetric positive-definite inertial matrix, $\mathbf{F}(\mathbf{q}, \dot{\mathbf{q}}) \in \mathcal{R}^{2 \times 2}$ the coriolis/centrifugal matrix, and $\mathbf{G}(\mathbf{q}) \in \mathcal{R}^{2 \times 1}$ the vector of gravitational torques. In our study, the dynamic model of the closed-loop five-bar mechanism was derived based on the approach developed by Ghorbel et al. [5]. The detailed descriptions of the dynamic model can be found in [9]. The dynamic model is a second-order ordinal differential equation. The Runge–Kutta algorithm in Matlab is used to solve the dynamic model.

It has been shown by Li et al. [7] and Zhang et al. [13], that if the condition for the force balancing is satisfied, the gravitational torques in Eq. (18) will vanish from the dynamic model, which makes sense of a simple dynamic model. Therefore, the dynamic model, both for the CW and the AKP approach, can be simplified as:

$$\mathbf{M}(\mathbf{q})\ddot{\mathbf{q}} + \mathbf{F}(\mathbf{q}, \dot{\mathbf{q}})\dot{\mathbf{q}} = \mathbf{T}(\mathbf{t}) \quad (19)$$

From the above dynamic model, one can see that when the mechanism is force balanced, the mechanism requires no input torque to remain in the position while the system is in its static state. Such characteristic can increase energy efficiency, improve accuracy and precision in positioning, and facilitating the design of a controller.

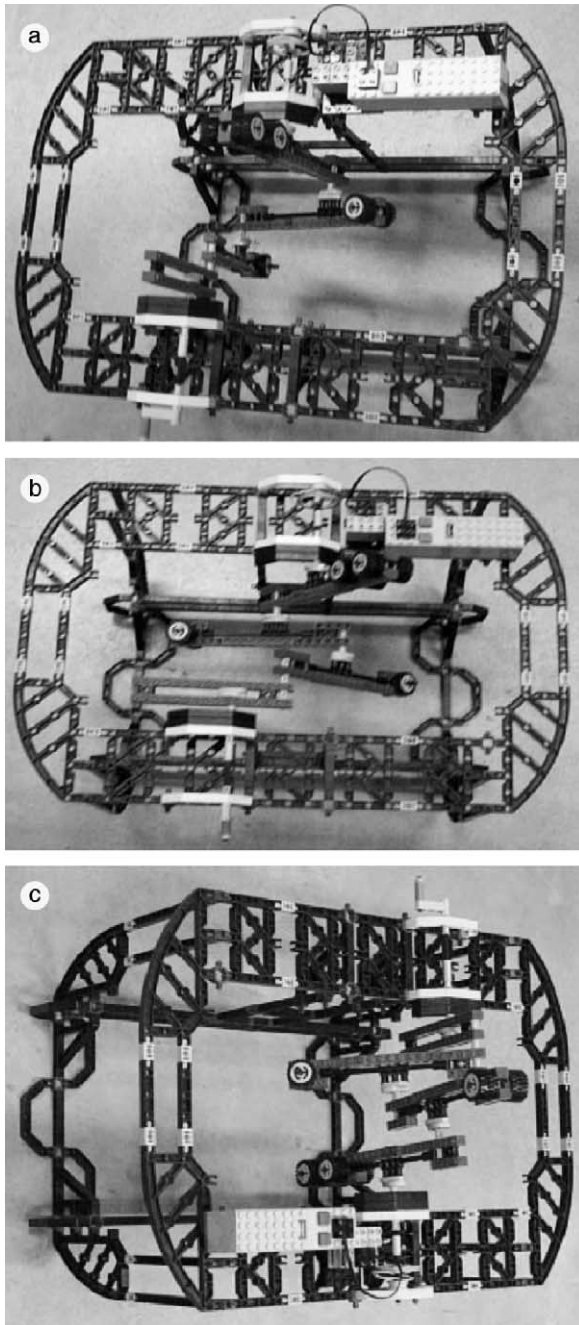


Fig. 3. (a) The unbalanced mechanism, (b) the balanced mechanism using the AKP approach (1), (c) the balanced mechanism using the AKP approach (2).

3.2. Control system

It is well known that the most current industrial manipulators are equipped with simple controllers such as PD or PID, which have been proven to be effective trajectory tracking controllers [3]. So in our studies, the following simple PD control algorithm is applied to control the closed-loop five-bar mechanism.

$$\mathbf{T}(t) = \mathbf{K}_P \mathbf{q}_e(t) + \mathbf{K}_D \dot{\mathbf{q}}_e(t) \tag{20}$$

where $\mathbf{T}(t)$ is the driving torque vector generated by the controller; \mathbf{K}_P and \mathbf{K}_D are the proportional and derivative gain matrix, respectively. $\mathbf{q}_e(t) = \mathbf{q}^d(t) - \mathbf{q}(t)$ represents the performance error appeared in the input angles, with $\mathbf{q}^d(t)$ as the desired angles, and $\dot{\mathbf{q}}_e(t)$ the angular velocity error vector of the input links.

Although PD controllers provide, in industrial environments, a cost/benefit performance that is difficult to beat with other kinds of controllers, it is not easy to use a fixed-gain PD controller to achieve a high dynamic performance with the substantial changes in operating conditions or environments. For these situations, the non-linear PD (NPD) controller is employed which can be viewed as the PD controller with non-constant gains.

A NPD controller may be in any form of control structures:

$$\mathbf{T}(t) = \mathbf{K}_P(\cdot) \mathbf{q}_e(t) + \mathbf{K}_D(\cdot) \dot{\mathbf{q}}_e(t) \tag{21}$$

where $\mathbf{K}_P(\cdot)$ and $\mathbf{K}_D(\cdot)$ are the time-varying proportional and derivative gain matrices. The non-linear gain function for the NPD controller in Eq. (21) is not unique. In our study, we use the following functions for the non-linear gains.

$$\begin{aligned} \mathbf{K}_P(\cdot) &= \mathbf{K}_{P0} \times \mathbf{K}(t) \\ \mathbf{K}_D(\cdot) &= \mathbf{K}_{D0} \times \mathbf{K}(t) \end{aligned} \tag{22}$$

where $\mathbf{K}(t) = \mathbf{K}_{\max} - \mathbf{K}_{\min} \operatorname{sech}(\mathbf{alf} \times \mathbf{q}_e(t))$. \mathbf{K}_{\max} , \mathbf{K}_{\min} , and \mathbf{alf} are user-defined positive constants. The gain $\mathbf{K}(t)$ is now upper-bounded by \mathbf{K}_{\max} when the error is infinite, and low-bounded by $\mathbf{K}_{\max} - \mathbf{K}_{\min}$ when the error is zero.

3.3. Inverse kinematics

The ability to control a mechanism remotely in real time hinges on the inverse kinematic solution—namely, given the position of the end-effector (O_3 in Fig. 1), i.e., point (x, y) , can the joint angles be determined? To the closed-loop five-bar mechanism, for links l_1 and l_2 , we have the following equations:

$$\begin{cases} l_1 \sin(q_1) + l_2 \sin(q_2) = y \\ l_1 \cos(q_1) + l_2 \cos(q_2) = x \end{cases} \tag{23}$$

Solving these equations, we can get:

$$q_2 = \tan^{-1} \left(\frac{ym_x - xm_y}{ym_x + xn_y} \right) \tag{24}$$

$$q_1 = q_2 + \Delta \tag{25}$$

where

$$\Delta = \cos^{-1} \left(\frac{x^2 + y^2 - l_1^2 - l_2^2}{2l_1l_2} \right), \quad m_x = l_1 \cos \Delta + l_2, \quad n_x = l_1 \sin \Delta, \\ m_y = n_x, \quad n_y = m_x$$

Two other angles q_3 and q_4 can be derived similarly. For details, see [11].

3.4. Motion planning

Once the joint angles are obtained through the inverse kinematics, a smooth function can be found for each of the two motors that passes through all via points and ends at the goal point; i.e., the trajectory is generated. A common way of driving a mechanism to move from here to there in a smooth, controlled fashion is to cause each point to drive as specified by a smooth function of time. In our study, the parametric quintic polynomials curve segment is used to produce the trajectories of the two actuators, and it can be expressed as:

$$q_i(t) = a_{0i} + a_{1i}t + a_{2i}t^2 + a_{3i}t^3 + a_{4i}t^4 + a_{5i}t^5 \quad t \in [0, t_i] \quad (26)$$

where q_i is the angle of the input link l_i . a_{0i} to a_{5i} are the coefficients for the quintic polynomials and t_i is the time of the input link moving in the i th spline segment. These coefficients can be determined according to the boundary conditions.

4. Results and discussion

To investigate the effectiveness of the AKP approach, simulation studies are carried out for the closed-loop five-bar mechanism. The parameters of the mechanism under different situations are listed in Table 1. Original (ORG) case describes the unbalanced mechanism shown in Fig. 1. In Appendix A, the design of mass redistribution for complete balancing of forces using the CW approach is presented. The CW case shows the parameters of the force balancing mechanism using the CW approach. The parameters of the mechanism using the AKP approach are shown in the AKP case. From Table 1, one can see that both the mechanism parameters and the inertia of AKP are significantly different from those of the CW approach.

Suppose that the end-effector (O_3 in Fig. 1) of the closed-loop five-bar mechanism passes a set of desired points; the coordinates of these points are listed in Table 2. In the present study, the end-effector of the mechanism in each case is required to pass all these points under the same initial conditions. According to the inverse kinematics of the mechanism, one can calculate the angular variables for two input links 1 and 4. The trajectories can be planned using the motion planning and are shown in Fig. 4.

As described in the previous section, from Fig. 4, it can be seen that the trajectories are not the same between the AKP approach and the CW approach.

Table 1
Parameters for AKP, CW and unbalanced structures used in the simulation

Parameters	ORG mechanism	CW mechanism	AKP mechanism
l_1 (m)	0.2	0.2	0.1
l_2 (m)	0.3	0.3	0.3
l_3 (m)	0.4	0.4	0.24
l_4 (m)	0.3	0.3	0.1
l_5 (m)	0.3	0.3	0.3
r_1 (m)	0.05	0.05	0.05
r_2 (m)	0.15	0.15	0.15
r_3 (m)	0.08	0.1	0.08
r_4 (m)	0.1	0.1875	0.1
m_1 (kg)	0.25	0.5	0.25
m_2 (kg)	0.25	0.25	0.25
m_3 (kg)	0.375	0.5	0.375
m_4 (kg)	0.5	1.0	0.5
I_1 (kg m ²)	0.004	0.01	0.004
I_2 (kg m ²)	0.01	0.01	0.01
I_3 (kg m ²)	0.02	0.035	0.02
I_4 (kg m ²)	0.02	0.038	0.02
θ_1 (rad)	0	π	π
θ_2 (rad)	0	0	0
θ_3 (rad)	0	π	π
θ_4 (rad)	0	π	π

Table 2
The coordinates of the via points of the end-effector

	0.35	0.30	0.25	0.15	0.04
x-axis (m)					
y-axis (m)	0.15	0.20	0.25	0.20	0.20

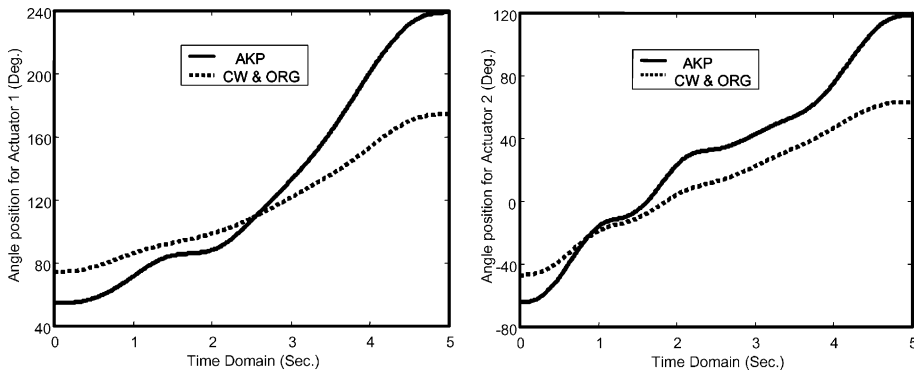


Fig. 4. The planned trajectories for the two actuators at the low speeds. Note: The trajectories for the two actuators at high speeds have the same shape except the time domain being the range of [0, 0.02].

4.1. Case 1: Trajectory tracking at low speeds

In this case, the time spans between two neighbouring points are 1.25, 1.0, 1.25, and 1.5 s, respectively. The average speeds of two servomotors are less than 6 rpm, so two servomotors are running at low speeds. The joint forces for the two actuators are calculated and illustrated in Fig. 5.

Via trail and error, the control gains of K_P are selected to be diagonal with the first element 600 and the second 750. The control gains of K_D are also selected to be diagonal with the first element 78 and the second 96. The simulation results are illustrated in Fig. 6, where the solid lines indicate the results of AKP case, the dashed-dotted lines indicate the results of the CW case, and the dotted lines represent the results of the ORG (unbalanced) case.

From the simulation results, it is observed that when the system runs at low speeds, after applying the force balancing, the motion tracking performance of the system is significantly improved using either the CW approach or the AKP approach. Fig. 6 shows that the tracking errors of the position and velocity are reduced in the CW approach, and are further reduced in the AKP approach. The fluctuation

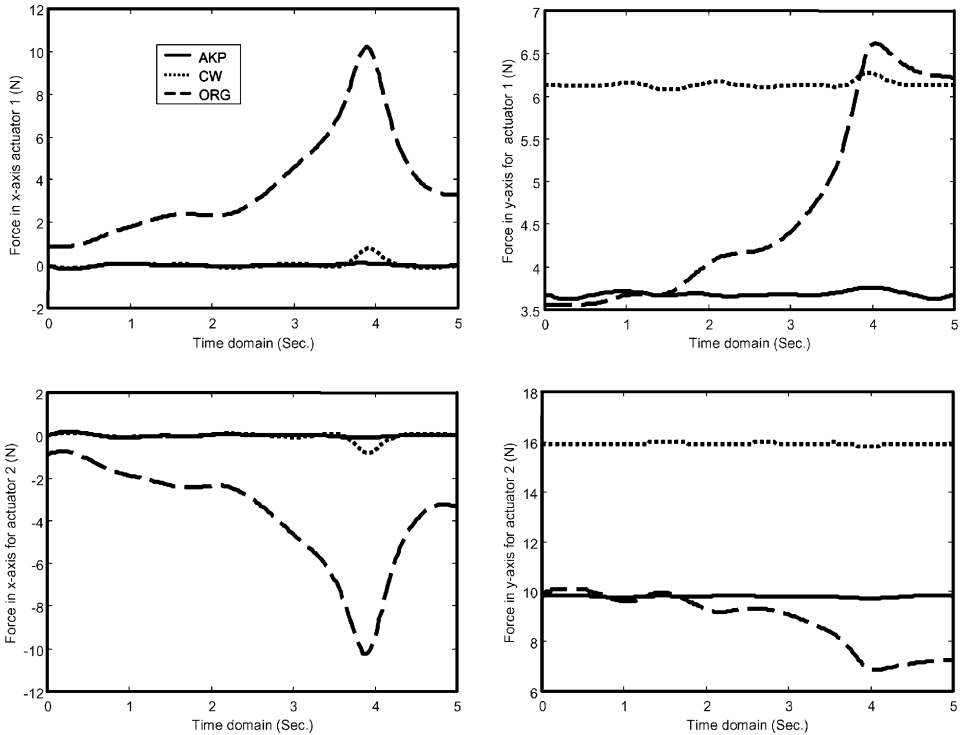


Fig. 5. Joint forces acted on two actuators for three cases at low speeds. Note: For all diagrams, the solid lines represent the AKP case; the dotted lines represent the CW case; and the dashed lines represent the ORG case.

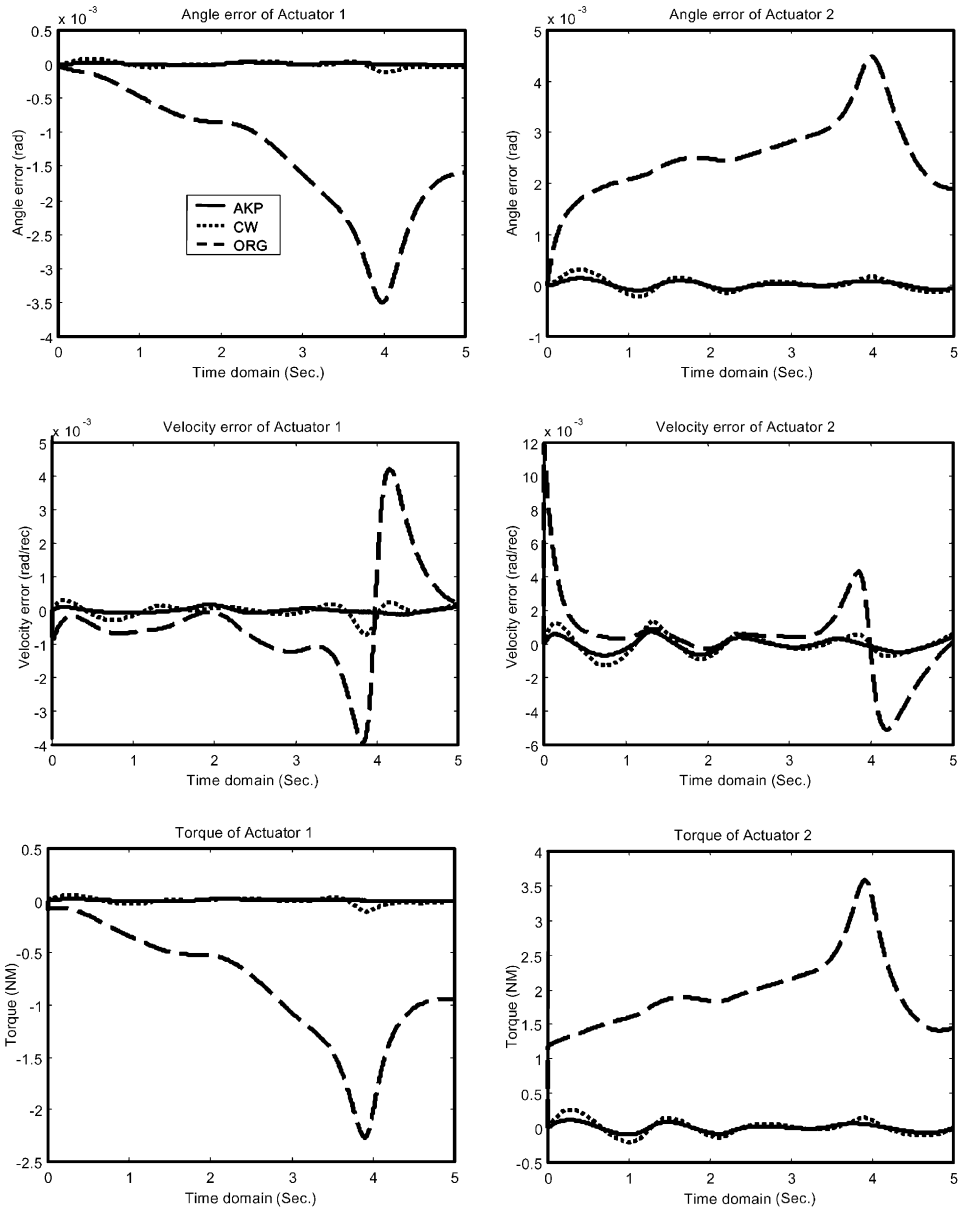


Fig. 6. The trajectory tracking performances of the five-bar mechanism at low speeds. Note: For all diagrams, the solid lines represent the AKP case; the dotted lines represent the CW case; and the dashed lines represent the ORG case.

of the tracking performance using the CW and AKP approaches is much smaller than that of the unbalanced mechanism. It is also shown from Fig. 6 that, after force balancing, the required torque in each servomotor is remarkably reduced comparing

with the unbalanced mechanism, so less energy is needed to operate the mechanism that is force balanced.

4.2. Case 2: Trajectory tracking at high speed

In this case, all via point positions of the end-effector are the same as in Table 2. The time spans passing via points are 0.05, 0.04, 0.05, and 0.06 s, respectively. The average speeds of the two motors reach about 100 rpm that means the mechanism is running at high speeds. Also, the joint forces for two actuators at high speeds are shown in Fig. 7.

Via trail and error, the control gains of K_P are selected to be diagonal with the first element 2000 and the second one 2500. The control gains of K_D are also selected to be diagonal with the first element 500 and the second one 700. The simulation results are illustrated in Fig. 8, where the lines have the same meanings as explained in the previous case.

As shown in Fig. 8, the performance of the AKP approach is the best among the three cases. The tracking errors, both angular errors and velocity errors of the two

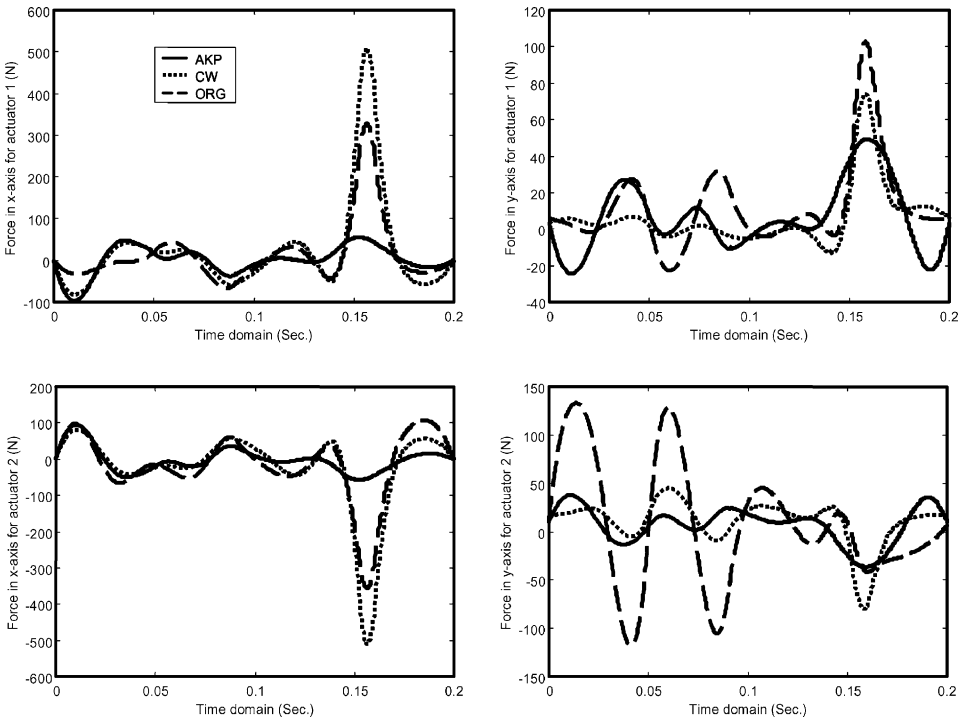


Fig. 7. Joint forces acted on two actuators for three cases at high speeds. Note: For all the diagrams, the solid lines represent the AKP case; the dotted lines represent the CW case; and the dashed lines represent the ORG case.

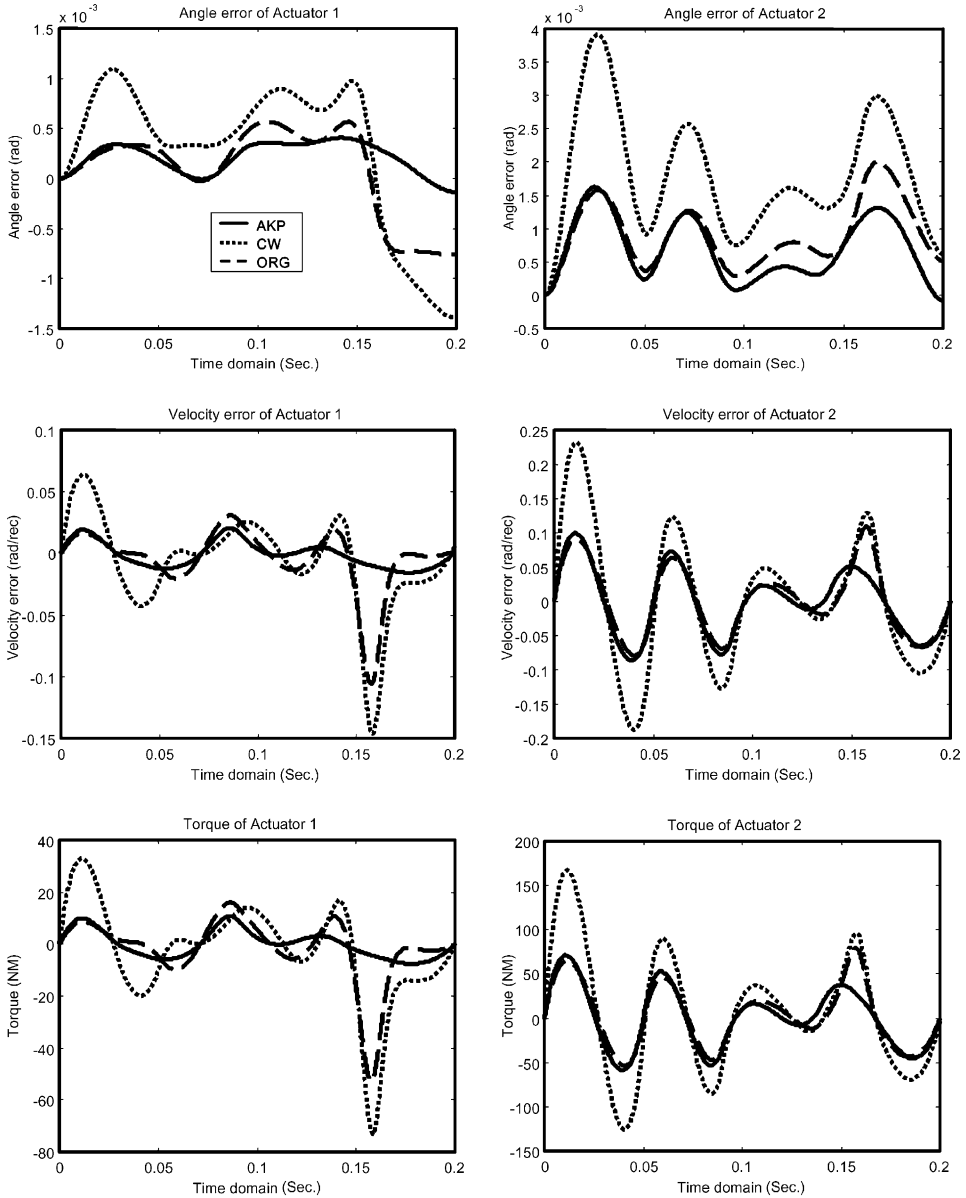


Fig. 8. The trajectory tracking performances of the five-bar mechanism at high speeds. Note: For all the diagrams, the solid lines represent the AKP case; the dotted lines represent the CW case; and the dashed lines represent the ORG case.

servomotors in the AKP approach, are the smallest. Moreover, the position control using the AKP approach is the best in each desired via points. It should be noticed that the performance of the CW approach is poorer than that of the unbalanced

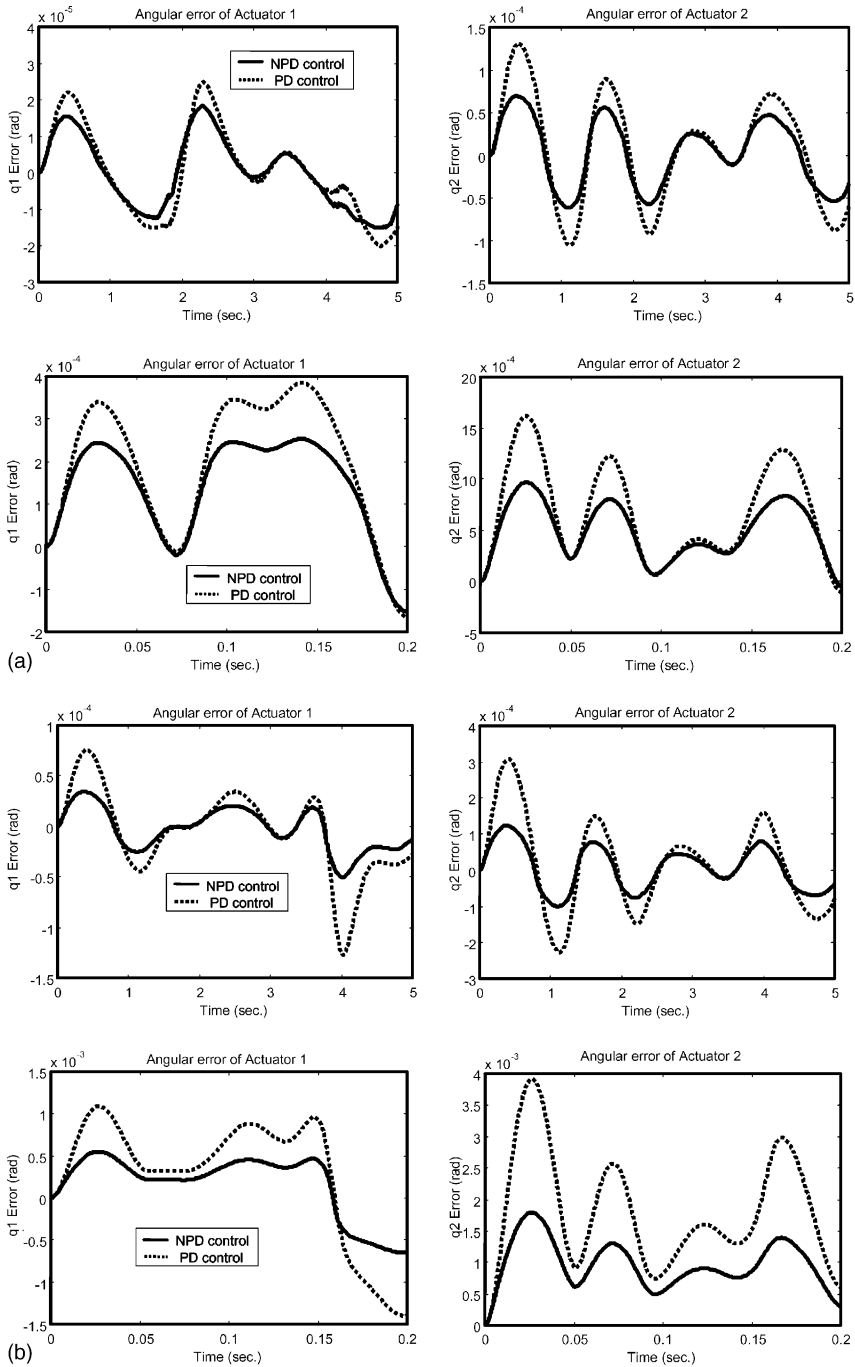


Fig. 9. PD and NPD controller vs. the CW approach and the AKP approach. (a) Using the AKP approach, (b) using the CW approach.

case. This means that when the mechanism runs at high speeds, the force balanced mechanism using the CW approach would decrease the tracking performance of the system. This phenomenon can be explained as follows: When the CW approach is used, both the mass and the inertia of the system are increased. The increase of mass and inertia means that the inertia forces of the links will be added. The larger the speed and acceleration of the mechanism, the bigger the adding inertia forces, and the more difficult the dynamic control of the mechanism. Mathematically, this means that the inertia matrix and the coriolis and centrifugal coefficient matrix increase in the dynamic model.

From Figs. 5 and 7, one can see that, when the mechanism runs at low speeds, the forces acting on the two actuators for the force balanced mechanism do not change very much, and the AKP approach can assure smaller forces at both the x -axis and the y -axis than the CW approach. But the forces for the unbalanced mechanism vary rapidly. But, when the mechanism runs at high speeds, the situation is totally different from the case at low speeds. First, the variations of the joint forces are very large for all three cases. These are caused by the large inertia forces acting on the actuators with the rapidly changed accelerations. Second, from these figures, we can see that the CW approach becomes the worst case at the x -axis, though the total forces of the two actuators in the x -axis are zero, and AKP approach obtains the best results.

Comparing Figs. 6 and 8, it should be noticed that, with the increase of the speed of the actuators, the tracking errors will increase for all three cases, but the increase of the tracking errors using the CW approach is the largest among three cases.

Furthermore, the NPD control is used to test the effectiveness of the AKP approach and the results are shown in Fig. 9. From Fig. 9, it can be seen that the NPD controller has more benefits in the reduction of trajectory tracking errors than the fixed-gain PD controller. Better performances for both the AKP and CW approaches can be obtained, and the AKP approach is more promising than the CW approach.

5. Conclusion

In this paper, a new force balancing method called AKP approach is presented and applied to the trajectory tracking of a closed-loop five-bar mechanism. The AKP approach cannot only build a force balanced mechanism, but also lead to the simplification of the dynamic model of a mechanism, and improve the tracking performance as well. Simulation studies show that the AKP approach can get a better tracking performance both in low speeds and high speeds than the CW approach and unbalanced mechanism. The AKP approach is more promising in terms of the reduction of joint forces than the CW approach. It is especially worth to point out that, after the force balancing using the AKP approach, the dynamic performance of the mechanism is improved, and less control energy is required. the AKP approach greatly facilitates the control of a force balanced mechanism for its generic task of tracking trajectories. The effect of force balancing on the closed-loop five-bar

mechanism vibrations is a future research work; also the optimal selection of adjusting parameters in the AKP approach is worth further study.

Acknowledgements

This research is supported by the Natural Sciences and Engineering Research Council (NSERC) of CANADA through a research grant awarded to the third author. The authors want to thank Kirk Backstrom to design and construct the prototype system using lego blocks.

Appendix A

The minimum number of the CWs needed to balance the closed-loop five-bar mechanism is 3 [3]. For convenience, the three CWs are usually attached to the fixed pivots of the two input links (Links 1 and 4) and a coupler Link 3. Only Link 2 remains unchanged; i.e., we can prescribe the parameters of Link 2 as $m_2 = m_2^0$ and $r_2 = r_2^0$, where the superscript 0 indicates the parameters of the unbalanced mechanism. According to the balancing conditions, the parameters of Links 1, 3, and 4 can be obtained from Eqs. (9)–(11), and, accordingly, the parameters of the counterweights can be acquired as:

$$m_i^* r_i^* e^{i\theta_i^*} = m_i^0 r_i^0 e^{i\theta_i^0} - m_i r_i e^{i\theta_i} \quad (i = 1, 3, 4) \tag{A.1}$$

where m_i^0 , r_i^0 , and θ_i^0 are the parameters of unbalanced mechanism, m_i^* , r_i^* , and θ_i^* are the parameters of the CWs, and m_i , r_i , and θ_i are the parameters after adding or deducting the CWs.

Apparently, in general, either m_i^* or r_i^* is arbitrarily selected, and the others accordingly obtained from Eq. (A.1).

References

- [1] Berkof RS, Lowen GG. A new method for completely force balancing simple linkages. *Trans ASME J Eng Ind* 1969;91(B):21–6.
- [2] Chuenchom T, Kota S. Synthesis of programmable mechanisms using adjustable dyads. *Trans ASME, J Mech Des* 1997;119(2):232–7.
- [3] Craig JJ. *Introduction to robotics*. 2nd ed. Reading, MA: Addison-Wesley; 1989.
- [4] Davies TH. *The kinematics and design of linkages: balancing mechanisms and machines*. *Mach Des Eng* 1968;6(3):40–51.
- [5] Ghorbel F, Chetelat O, Longchamp R. A reduced model or constrained rigid bodies with application to parallel robots. In: *Proceedings of the 4th IFAC symposium on robot control*, Capri, Italy, September 1994.
- [6] Gosselin CM. Static balancing of spherical 3-DoF parallel mechanisms and manipulators. *Int J Rob Res* 1999;18(8):819–29.
- [7] Li Q, Tso SK, Guo LS, Zhang WJ. Improving motion tracking of servomotor driven closed-loop mechanisms using mass-redistribution. *Mech Mach Theory* 2000;35(7):1033–45.

- [8] Lowen GG, Tepper FR, Berkof RS. Balancing of linkages—an update. *Mech Mach Theory* 1983;18(3):213–20.
- [9] Ouyang PR, Zhang WJ, Wu FX. Nonlinear PD control for trajectory tracking with consideration of the design for control methodology. In: 2002 IEEE International Conference on Robotics and Automation, Washington DC, May 11–15, 2002.
- [10] Papadopoulos E, Abu-Abed A. On the design of zero reaction manipulators. *Trans ASME, J Mech Des* 1996;118(3):372–6.
- [11] Ouyang PR. Force balancing design and trajectory tracking control of real-time controllable mechanisms. M.Sc. thesis, University of Saskatchewan, 2002.
- [12] Youcef-Toumi K, Kuo ATK. High-speed trajectory control of a direct-drive manipulator. *IEEE Trans Rob Autom* 1993;9(1):102–8.
- [13] Zhang WJ, Li Q, Guo LS. Integrated design of mechanical structure and control algorithm for a programmable four-bar linkage. *IEEE/ASME Trans Mech* 1999;4(4):354–62.
- [14] Zhang WJ, Zou J, Watson G, Zhao W, Zhong GH, Bi SS. Constant Jacobian method for kinematics of a 3-DOF planar micro-motion stage. *J Rob Syst* 2002;19(2):63–79.